

## **A highly active molybdenum multisulfide electrocatalyst for hydrogen evolution reaction**

Li-Fang Zhang,<sup>ab</sup> Gang Ou,<sup>b</sup> Liu Gu,<sup>c</sup> Zhi-Jian Peng,<sup>c</sup> Lu-Ning Wang<sup>\*a</sup> and Hui Wu<sup>\*b</sup>

<sup>a</sup>Laboratory of Advanced Healthcare Materials, School of Materials Science and Engineering, University of Science and Technology Beijing, Beijing 100083, P. R. China

<sup>b</sup>State Key Laboratory of New Ceramics and Fine Processing, School of Materials Science and Engineering, Tsinghua University, Beijing 100084, P. R. China

<sup>c</sup>School of Engineering and Technology, China University of Geosciences, Beijing 100083, P.R. China

## Experimental Details

**Preparation of the A-MoS<sub>x</sub> materials:** Firstly, the original MoS<sub>2</sub> powders (99.9%) were pressed into pellets and then were arc-melting treated in the closed arc furnace filled with Ar. During the treatment, the MoS<sub>2</sub> pellets were rapidly heated up to a very high temperature (>3000 °C) and melted, then cooled to room temperature within a few seconds on a copper substrate, which was kept thermostatic at 15 °C. The as-prepared black particles were ground to powders, followed by ball-milling for 4 h. Then, the A-MoS<sub>x</sub> catalysts were obtained.

**Electrochemical measurement:** All of the electrochemical measurements were performed on CHI 660E electrochemical workstation in three-electrode systems. Typically, 4 mg of sample and 30 μL Nafion solution (5 wt %) were dispersed in 1 mL water-ethanol solution with volume ratio of 3:1 by sonicating for 30 min to form a homogeneous ink, then the mixed ink were attached onto a glass carbon (GC) electrode with 4 mm diameter (loading 2.1 mg cm<sup>-2</sup>) as working electrode, polished with alumina slurry and cleaned with ethanol and DI water before experiment. A graphite rod and Ag/AgCl (in saturated KCl solution) electrode were used as counter and reference electrodes, respectively. All of the potentials were calibrated to a reversible hydrogen electrode (RHE). Linear-sweep voltammetry (LSV) measurements were conducted in 0.5 M H<sub>2</sub>SO<sub>4</sub> and 1.0 M KOH at scan rates from 5 mV s<sup>-1</sup> to 300 mV s<sup>-1</sup>. All data have been corrected for a small ohmic drop based on impedance spectroscopy. The electrochemical impedance spectroscopy (EIS) measurements were carried out in the same configuration at overpotential of 0 mV from 10<sup>5</sup> to 0.1 Hz with an AC voltage of 5 mV.

**Characterization:** The morphology of the prepared samples was investigated by scanning electron microscopy (SEM, MERLIN VP Compact, Carl Zeiss, Germany) and transmission electron microscopy (TEM, JEM-2010). X-ray diffraction (XRD) patterns were obtained by using a D/max-2500 diffractometer with a Cu K $\alpha$  irradiation source ( $\lambda=1.54$  Å). X-ray photoelectron spectroscopy (XPS) data were obtained with an ESCALAB 250Xi from Thermo Fisher Scientific electron spectrometer using an Al K $\alpha$  radiation. The particle size of samples was measured by laser scattering particle analyzer (Hydro 2000NW, MALver, Worcestershire, UK). Photoluminescence spectra and Raman spectra were measured on a microscopic confocal Raman spectrometer (Raman, LabRAM HR800, HORIBA Jobin Yvon, Villeneuve d'Ascq, France) using a 514 nm laser as the excitation source.

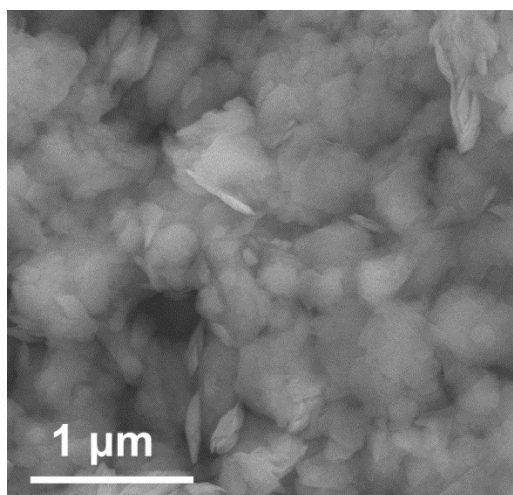


Fig. S1 SEM image of MoS<sub>2</sub>.

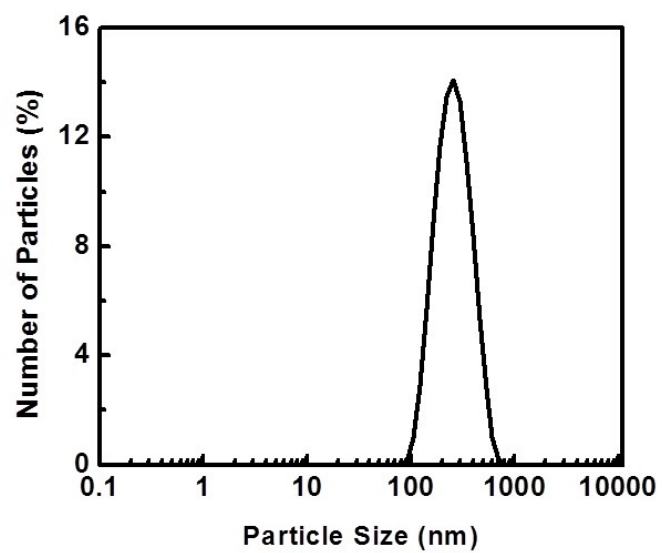


Fig. S2 Particulate size analysis of the MoS<sub>2</sub>.

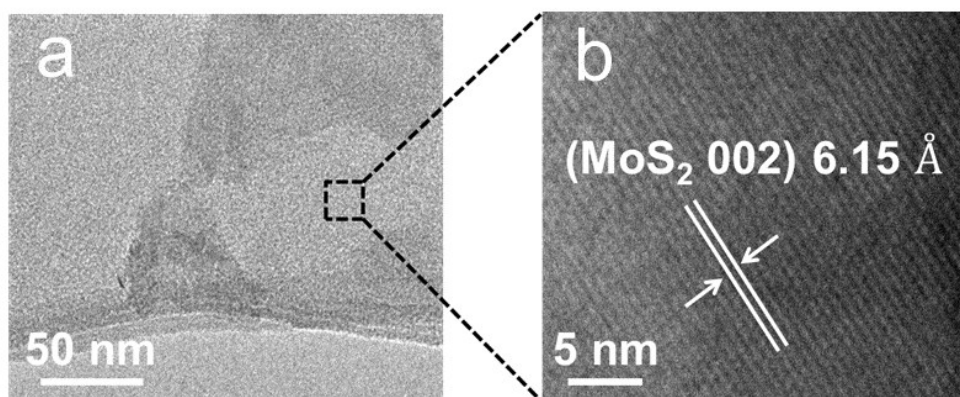


Fig. S3 (a) TEM image of MoS<sub>2</sub>. (b) HRTEM image of MoS<sub>2</sub>.

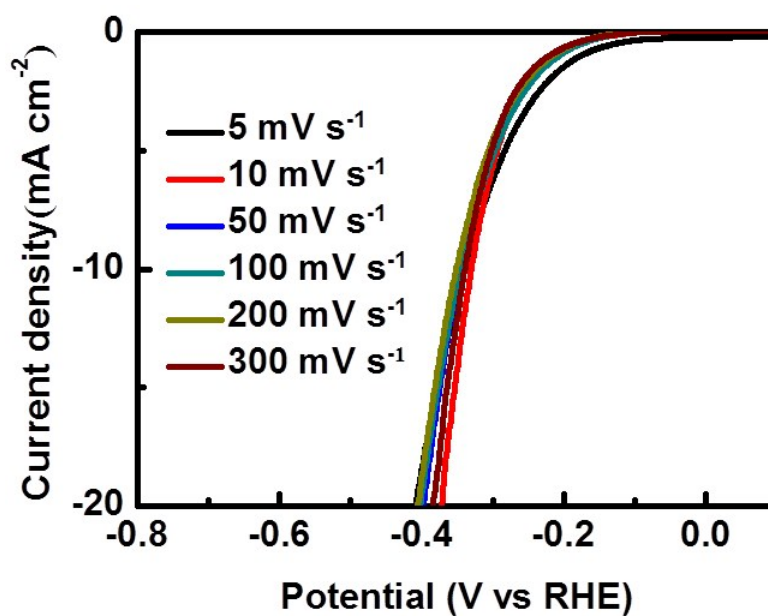


Fig. S4 The polarization curves of the MoS<sub>2</sub> with scan rates from 5 to 300 mV s<sup>-1</sup> in 0.5 M H<sub>2</sub>SO<sub>4</sub>.

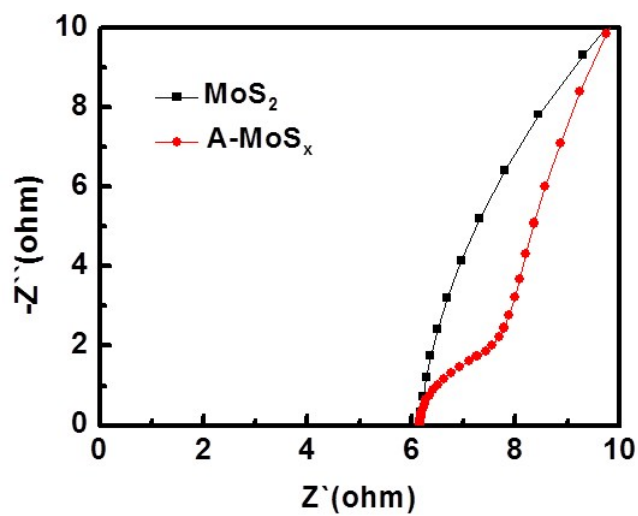


Fig. S5 Electrochemical impedance spectra of the  $\text{A-MoS}_x$  and  $\text{MoS}_2$  in 1.0 M KOH.

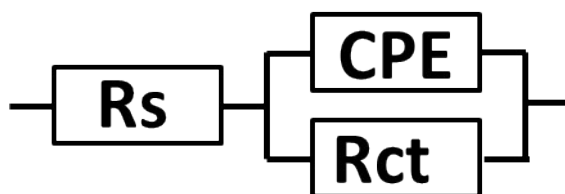


Fig. S6 The equivalent circuit used in EIS analysis.

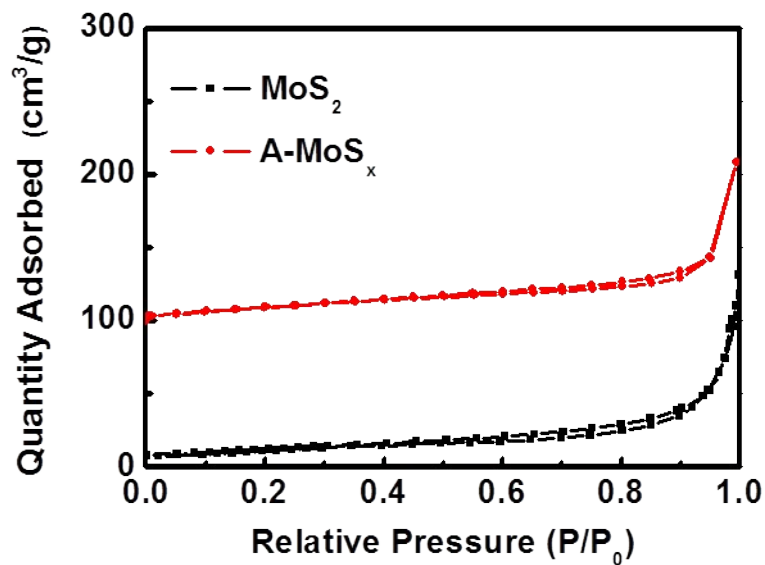


Fig. S7  $\text{N}_2$ -sorption isotherms of the  $\text{A-MoS}_x$  and  $\text{MoS}_2$ .

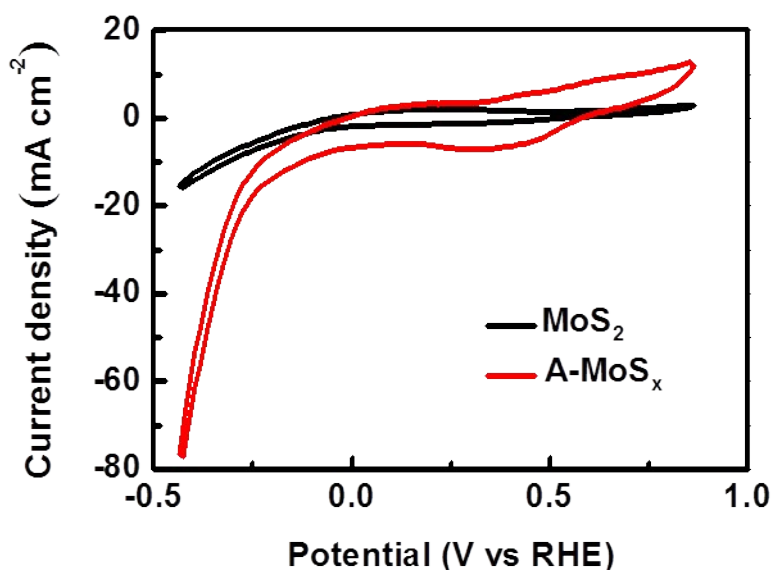


Fig. S8 The cyclic voltammetry (CV) curves of the A-MoS<sub>x</sub> and MoS<sub>2</sub> with a scan rate of 50 mV s<sup>-1</sup> in 0.5 M H<sub>2</sub>SO<sub>4</sub>.

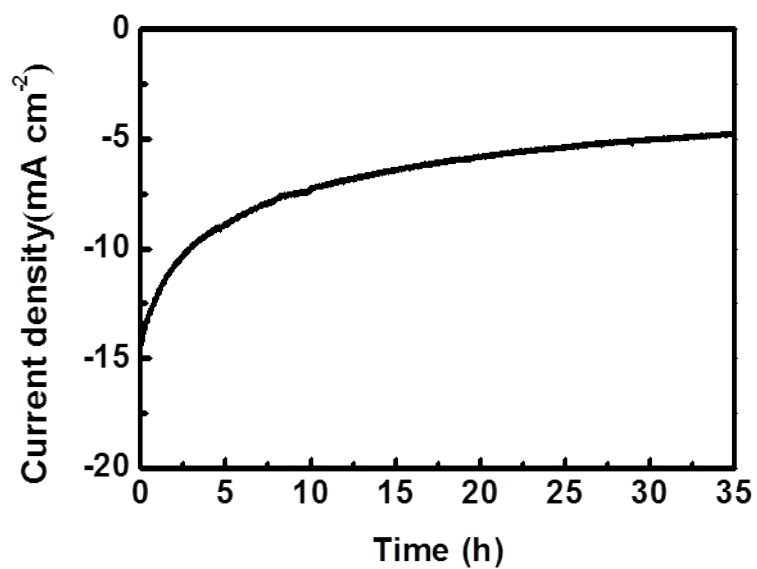


Fig. S9 Time-dependent HER performance of the A-MoS<sub>x</sub> in 0.5 M H<sub>2</sub>SO<sub>4</sub>.

**Table S1.** HER parameters of the typical comparable samples.

Sample	Electrolyte	Current density	Tafel slope (mV dec <sup>-1</sup> )	Ref.
A-MoS <sub>x</sub>	0.5M H <sub>2</sub> SO <sub>4</sub>	10 mA cm <sup>-2</sup> at η =156 mV	58	Our work
Double-gyroid MoS <sub>2</sub>	0.5M H <sub>2</sub> SO <sub>4</sub>	10 mA cm <sup>-2</sup> at η =260 mV	60	S1
Chemically exfoliated 1T- MoS <sub>2</sub>	0.5M H <sub>2</sub> SO <sub>4</sub>	10 mA cm <sup>-2</sup> at η≈187	43	S2
MoS <sub>2</sub> /graphene hybrid	0.5M H <sub>2</sub> SO <sub>4</sub>	10 mA cm <sup>-2</sup> at η≈140mV	41	S3
Defect-rich ultrathin MoS <sub>2</sub>	0.5M H <sub>2</sub> SO <sub>4</sub>	13 mA cm <sup>-2</sup> at η=200 mV	50	S4
Vertically aligned MoS <sub>2</sub> films	0.5M H <sub>2</sub> SO <sub>4</sub>	8 mA cm <sup>-2</sup> at η=400 mV	86	S5
Strained vacancy MoS <sub>2</sub>	H <sub>2</sub> SO <sub>4</sub> (pH=2)	10 mA cm <sup>-2</sup> at η=170 mV	60	S6
MoS <sub>x</sub> from electro-polymerization	1M H <sub>2</sub> SO <sub>4</sub>	15 mA cm <sup>-2</sup> at η=200 mV	40	S7
Wet-Chemical amorp MoS <sub>x</sub>	1M H <sub>2</sub> SO <sub>4</sub>	10 mA cm <sup>-2</sup> at η≈200	60	S8
MoS <sub>x</sub> /N-CNT	0.5M H <sub>2</sub> SO <sub>4</sub>	10 mA cm <sup>-2</sup> at η=110 mV	40	S9
CoMoS <sub>x</sub>	H <sub>2</sub> SO <sub>4</sub> (pH=1)	5 mA cm <sup>-2</sup> at η≈210 mV	N/A	S10
MoO <sub>3</sub> - MoS <sub>2</sub>	0.5M H <sub>2</sub> SO <sub>4</sub>	10 mA cm <sup>-2</sup> at η≈250	50-60	S11
Nanowires		mV		
Defects Engineered Monolayer MoS <sub>2</sub>	0.5M H <sub>2</sub> SO <sub>4</sub>	10 mA cm <sup>-2</sup> at η≈590	161	S12

## Reference

- S1 J. Kibsgaard, Z. Chen, B. N. Reinecke, T. F. Jaramillo, *Nat. Mater.* 2012, **11**, 963.
- S2 M. A. Lukowski, A. S. Daniel, F. Meng, A. Forticaux, L. S. Li, S. Jin, *J. Am. Chem. Soc.* 2013, **135**, 10274.
- S3 Li, Y.; Wang, H.; Xie, L.; Liang, Y.; Hong, G.; Dai, H. *J. Am. Chem. Soc.* **2011**, *133*, 7296.
- S4 J. F. Xie, H. Zhang, S. Li, R. X. Wang, X. Sun, M. Zhou, J. F. Zhou, X. W. Lou, Y. Xie, *Adv. Mater.* 2013, **25**, 5807.
- S5 D. Kong, H. Wang, J. J. Cha, M. Pasta, K. J. Koski, J. Yao, Y. Cui, *Nano Lett.* 2013, **13**, 1341.
- S6 H. Li, C. Tsai, A. L. Koh, L. Cai, A. W. Contryman, A. H. Fragapane, J. Zhao, H. S. Han, H. C. Manoharan, F. Abild-Pedersen, J. K. Nørskov, X. Zheng, *Nat. Mater.* 2016, **15**, 48.
- S7 D. Merki, S. Fierro, H. Vrubel, X. Hu, *Chem. Sci.* 2011, **2**, 1262.
- S8 J. D. Benck, Z. Chen, L. Y. Kuritzky, A. J. Forman, T. F. Jaramillo, *ACS Catal.* 2012, **2**, 1916.
- S9 D. J. Li, U. N. Maiti, J. Lim, D. S. Choi, W. J. Lee, Y. Oh, G. Y. Lee, S. O. Kim, *Nano Lett.* 2014, **14**, 1228.
- S10 J. Staszak-Jirkovský, C. D. Malliakas, P. P. Lopes, N. Danilovic, S. S. Kota, K. C. Chang, B. Genorio, D. Strmcnik, V. R. Stamenkovic, M. G. Kanatzidis, N. M. Markovic, *Nat. Mater.* 2016, **15**, 197.
- S11 Z. Chen, D. Cummins, B. N. Reinecke, E. Clark, M. K. Sunkara, T. F. Jaramillo, *Nano Lett.* 2011, **11**, 4168.
- S12 G. Ye, Y. Gong, J. Lin, B. Li, Y. He, S. T. Pantelides, W. Zhou, R. Vajtai, P. M. Ajayan, *Nano Lett.* 2016, **16**, 1079.